Atomic Scale Sliding and Rolling of Carbon Nanotubes

A. Buldum* and Jian Ping Lu†

Department of Physics and Astronomy, The University of North Carolina at Chapel Hill, Chapel Hill, North Carolina 27599
(Received 4 June 1999)

Using molecular statics and dynamics methods we investigate the motion of nanotubes on a graphite surface. Each nanotube has unique equilibrium orientations with sharp potential energy minima which lead to atomic scale locking of the nanotube. The effective contact area and the total interaction energy scale with the square root of the radius. Sliding and rolling nanotubes have different characters. The potential energy barriers for sliding nanotubes are higher than that for perfect rolling. When the nanotube is pushed, we observe a combination of atomic scale spinning and sliding motion.

Although the fundamental aspects of friction have been studied for more than centuries, our knowledge about its microscopic aspects is very limited [1]. The invention of atomic force microscope (AFM) [2] and its application in measurements of atomic scale friction [3] [friction force microscope (FFM)] have made a great impact on the studies of friction. A carbon nanotube is a stable nano-object having cylindrical shape [4], thus ideal for understanding atomic scale friction. Falvo *et al.* showed that it is possible to slide, rotate, and roll carbon nanotubes on a graphite surface [5]. They demonstrated that a nanotube has preferred orientations on the graphite surface and prefer rolling than sliding when it is in atomic scale registry with the surface. In this study, we carried out molecular statics, dynamics calculations, and studies of stick-slip motion for a variety of nanotubes. We found the following: (i) A nanotube has sharp potential energy minima leading to orientational locking. The locking angles are directly related to the chiral angle. (ii) Sliding and rolling nanotubes have different characters. The energy barriers for sliding are higher than the barriers for perfect rolling. (iii) The effective contact area and total interaction energy scale with the square root of the radius. (iv) A combination of sliding and spinning motion is observed when the tube is pushed. The net result is rolling with the friction force comparable to the corresponding force for sliding.

The character of interaction between the moving object (atom, molecule, or any nanoparticle) and the underlying surface defines the motion [6]. The interaction energy may consist of short-range, attractive interaction energy due to chemical bonding; short-range repulsive energy and long-range, attractive van der Waals energy. The interaction between a carbon nanotube and a graphite surface is similar to that between two graphite planes which is weak and van der Waals in origin. To investigate the overall behavior of the motion of a carbon nanotube on a graphite surface, we represent the interaction between the tube and the graphite surface atoms by an empirical potential of Lennard-Jones type [7] which was used extensively to study solid C_{60} and nanotube [8]. Recent theoretical calculations [9] showed that multiwall nanotubes on a

graphite surface are not deformed significantly. The atomic scale motion is determined mostly by the interaction of the outmost layer of the nanotube with the surface. In this work we studied rigid single wall nanotubes with different chiralities and radii.

The energy barriers related to the motion of nanotubes can be conveniently analyzed by calculating the variation of the potential energy, E_P, and corresponding force during the motion. Four different types of motion are considered: spinning, rotating, sliding, and rolling. During each step of motion the height of the tube is optimized. We first spin and rotate the nanotubes in order to find the equilibrium positions. Figure 1 shows the interaction energy as a function of the rotation angle between the tube axis and the graphite lattice (all the data given in this study is for per Å length of the nanotubes). Each nanotube has unique equilibrium orientations repeating in every 60°, reflecting the lattice symmetry of the graphite. The variation of energy near the minimum is very sharp which causes atomic scale locking of the nanotube. Locking angles are different for different nanotubes, and they
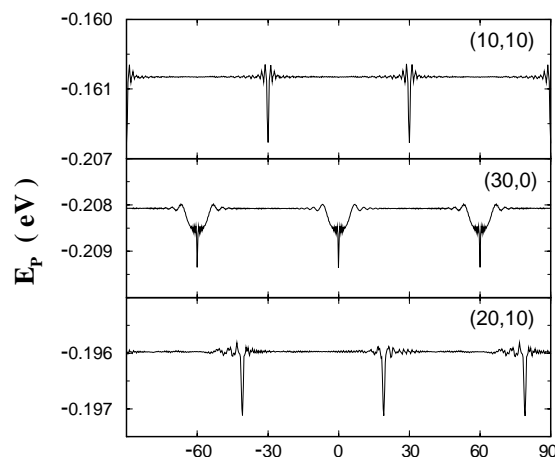

FIG. 1. The interaction energy as a function of rotation angle between the nanotube axis and the graphite lattice for (10, 10), (30, 0), and (20, 10) nanotubes. Each nanotube has unique minimum energy orientations repeating in every 60°.

    0031-9007/99/83(24)/5050(4)$15.00

are the direct measure of the chiral angle. This provides a novel method for measuring the chiralities of carbon nanotubes. Another important point in Fig. 1 is that the energy variation between two consecutive energy minima is very small (except near the minima). Thus the force needed to rotate a nanotube is very small when the tube is out-of-registry. These results are in good agreement with the recent experiments by Falvo et al. [5].

Next, we studied sliding and rolling of carbon nanotubes. In Fig. 2(a) the variation of the total interaction energy $E_P(s)$ of a $(20, 10)$ nanotube as a function of sliding distance s is shown. The energy variation is very small for rolling since perfect atomic scale registry is always maintained in the contact region. On the other hand, in sliding motion, all the atoms in the contact region move simultaneously out-of-registry to higher energy positions and contribute to the energy barrier of motion. When the nanotube is attached to an AFM tip, stick-slip motion occurs. The tube first sticks and then slips suddenly (slides or rolls or both) when the force exerted by the tip is sufficiently large [10]. The friction force in stick-slip motion of the nanotube when it is attached to an AFM tip (with string constant $\sim 8.0 \times 10^{-3}$ N/m) is shown in Fig. 2(b). The area in the hysteresis curve gives us the amount of energy dissipated during the stick-slip motion.
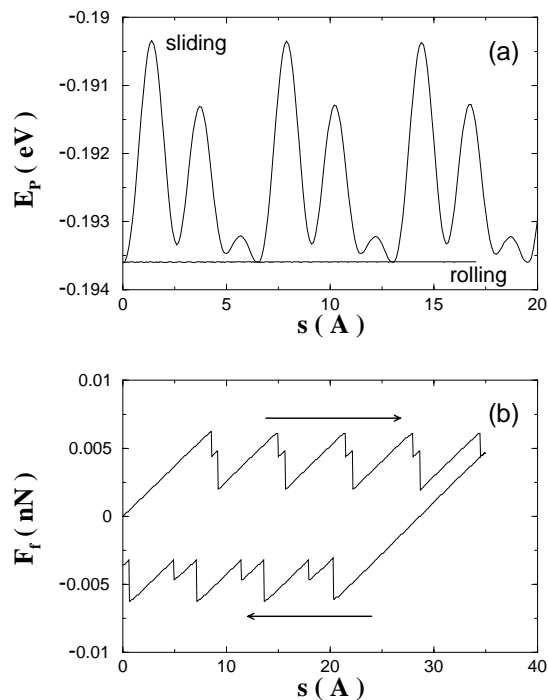
To investigate the tube dependence, we performed calculations with tubes in different chiralities or radii. Figure 3(a) shows the interaction energy as a function of the nanotube radius, R. We found that the effective contact area and the interaction energy scale with the square root of the radius of the nanotube. The interaction energy is independent of chirality. In-registry sliding force (when the tube is in a minimum energy orientation) is also scaled with the square root of the radius. However, the sliding force is different for nanotubes with different chiralities and the same radii. Figure 3(b) shows the force for in-registry sliding and rolling. For a typical nanotube (radius ~ 13 nm, length ~ 600 nm), the sliding force value is estimated as ~ 87 nN for an armchair tube and ~ 43 nN for a zigzag tube, in good agreement with the friction force values measured in the experiments [5] (~ 50 nN).

The static calculations we discussed give insight of ideal sliding and rolling. However, the dynamical behavior is crucial for the competition between sliding and rolling in the course of motion. In our model, the graphite substrate and the nanotube are considered to be rigid, but the nanotube as a whole is able to move having translational and spinning degrees of freedom. Constant lateral force was applied to the nanotube for a short period of time (50 ps) and then the motion of the nanotube was analyzed. In the same way, we applied constant torque or combinations of torque and lateral force to the nanotube. The total energy of the system was kept constant.
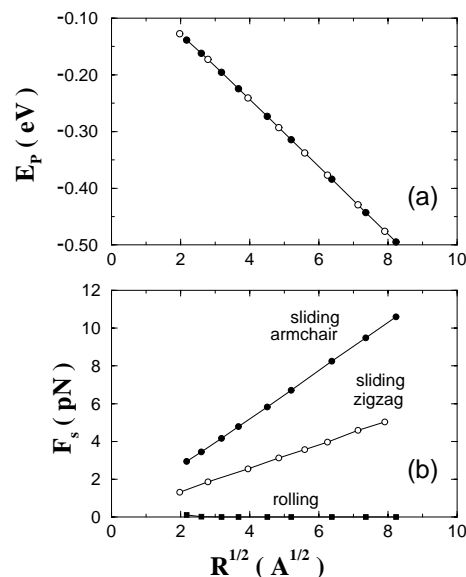

FIG. 2. (a) The variation of the interaction energy E_P of a $(20, 10)$ nanotube as a function of sliding and rolling distances. (b) The friction force in stick-slip motion of the $(20, 10)$ nanotube when attached to an AFM tip with spring constant $\sim 8.0 \times 10^{-3}$ N/m.

FIG. 3. (a) The interaction energy as a function of square root of the nanotube radius, $\sqrt{R}$. The filled circles correspond to armchair tubes, and the hollow circles correspond to zigzag tubes with different radii. (b) The corresponding force for in-registry sliding and rolling of the nanotubes as a function of $\sqrt{R}$.

After constant lateral force is applied on the nanotube, slide-spin motions in the atomic scale are observed [11]. When the atoms in the contact region are in atomic scale registry it is easier for the nanotube to slide. Then the nanotube atoms move from in-registry to out-of-registry positions and it is easier for the nanotube to spin. By spinning the nanotube decreases its potential energy and the atoms recover the in-registry positions. Switching of the tube motion between spinning and sliding can be clearly seen in the sliding and the spinning components of the kinetic energy shown in Fig. 4(a). The switching is in the atomic scale and directly related to the corrugation of interaction energy. The total force acting on the tube in the direction of motion is shown in Fig. 4(b). The maximum value of the force is comparable to the force required to slide the nanotube [see Fig. 3(b)]. Sliding and spinning distances (angle multiplied by R) as functions of time are shown in Fig. 4(c). Ideal rolling would be a perfect overlap of sliding and spinning distances; meanwhile slide-spin motion gives oscillations, and the net result is equivalent to rolling.

For a better understanding of the slide-spin motion, we plot the interaction energy as a function of sliding distance and spinning angle in Fig. 5(a). The trajectory for ideal rolling is a line at the bottom of the valleylike regions. However, a nanotube performing slide-spin motion follows an oscillating path in these valleys [see Fig. 5(b)] with an amplitude of oscillation depending on the initial kinetic energy.

When the system is coupled to a heat bath or energy dissipation due to friction is considered, there are changes in the slide-spin motion. We modeled the dissipation by additional velocity dependent forces [12] on the atoms close to the contact region. The results are presented in Fig. 6. Without energy dissipation the tube oscillates in the valleylike regions of potential energy surface [see Fig. 5(a)] in the slide-spin motion. When the energy dissipation is considered, the total kinetic energy decreased and there is more mixing between sliding and spinning. Eventually, the nanotube performs ideal rolling. If the nanotube has very high kinetic energy, it slides over many surface unit cells. But because of energy dissipation the tube's total kinetic energy decreases and slide-spin motion starts. Afterwards the motion is close to ideal rolling [as seen in Fig. 6(b)]. This atomic scale picture of rolling is very similar to the rolling of macroscopic objects. Recent molecular dynamics simulations [13] with a full relaxed system by Schall and Brenner find similar conclusions.
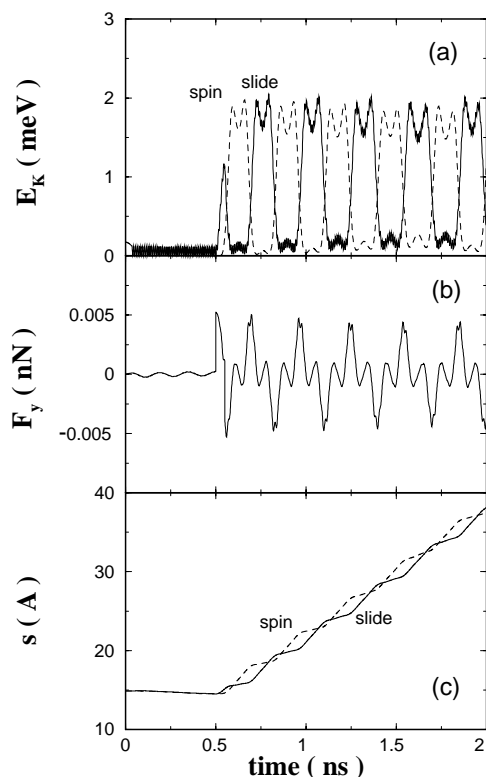

FIG. 4. (a) After the initial push, sliding and spinning components of the kinetic energy of the (10, 10) nanotube as functions of time are represented by the solid and dashed lines, respectively. Notice the switching between spinning and sliding motions in the atomic scale. (b) The total force acting on the tube in the direction of motion. (c) The sliding and spinning distances (angle multiplied by R) as functions of time.
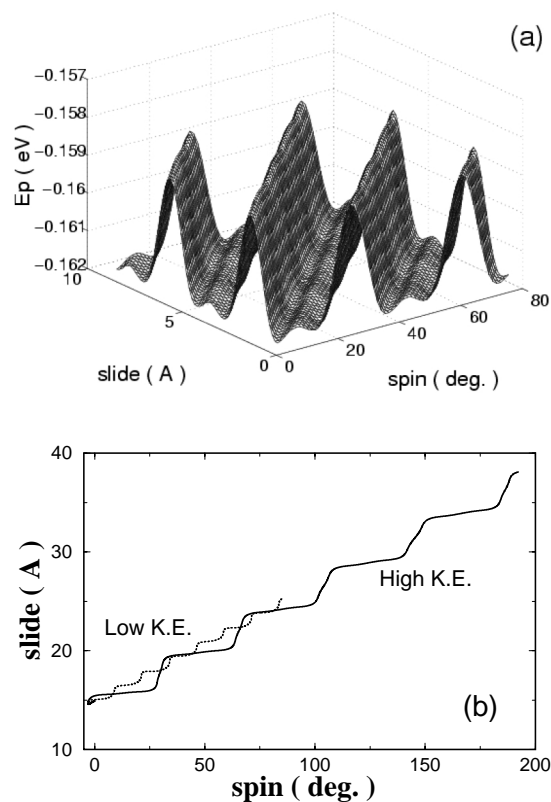

FIG. 5. (a) The variation of the interaction energy as a function of sliding distance and spinning angle. (b) The trajectories correspond to the slide-spin motion of a nanotube having lower and higher total kinetic energies on the plane defined in (a).
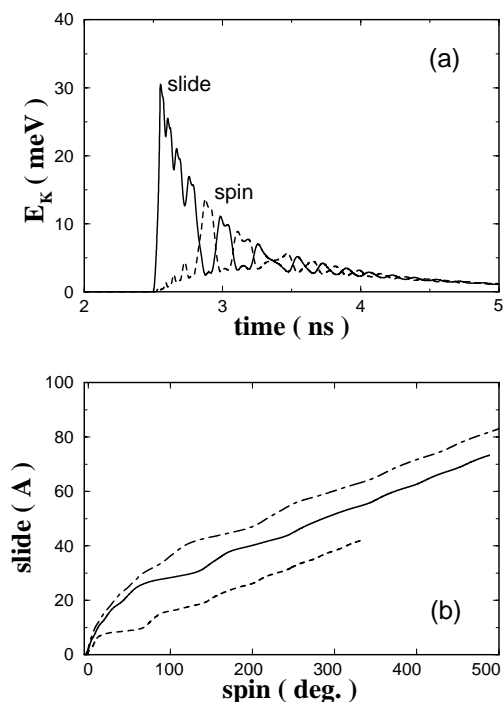
FIG. 6. (a) Sliding and spinning components of the kinetic energy of the $(10, 10)$ nanotube as functions of time are represented by the solid and dashed lines, respectively. (b) The nanotube's trajectories on the surface defined in Fig. 5(a) for different initial kinetic energies. The trajectories from higher to lower initial kinetic energies are represented by dot-dashed, solid, and dashed lines, respectively. The kinetic energy values in (a) correspond to the trajectory plotted by solid line.

To conclude, we investigated different types of motion of carbon nanotubes on a graphite surface. Each nanotube has unique minimum energy orientations with respect to the surface structure. The variation of interaction energy is very sharp leading to orientational locking of the nanotubes. The locking angles are a direct measure of the chiral angles, and this provides a novel method for measuring the nanotube chirality. The effective contact area and the total interaction potential energy scale with the square root of the radius of the nanotube. A combination of atomic scale spinning and sliding motion is observed when the nanotube is pushed.

   *Email address: buldum@physics.unc.edu
   [†]Email address: jpl@physics.unc.edu
[1] For a general review and references see B. Bhushan, J. N. Israelachvili, and U. Landman, Nature (London) **347**, 607 (1995); B. N. J. Persson, *Sliding Friction,* Springer Series in Nanoscience and Technology (Springer-Verlag, Berlin, 1998), p. 1.
[2] G. Binnig, C. F. Quate, and Ch. Gerber, Phys. Rev. Lett. **56**, 930 (1986).
[3] C. M. Mate, G. M. McClelland, R. Erlandsson, and S. Chiang, Phys. Rev. Lett. **59**, 1942 (1987).
[4] S. Ijima, Nature (London) **354**, 56 (1991); for a general review see R. Saito, G. Dresselhaus, and M. S. Dresselhaus, *Physical Properties of Carbon Nanotubes* (Imperial College Press, London, 1998); *Carbon Nanotubes: Preparation and Properties,* edited by T. W. Ebbesen (CRC, Boca Raton, 1997).
[5] M. R. Falvo, R. M. Taylor, A. Helser, V. Chi, F. P. Brooks, S. Washburn, and S. Superfine, Nature (London) **397**, 236 (1999).
[6] A. Buldum and S. Ciraci, Phys. Rev. B **54**, 2175 (1996); A. Buldum, S. Ciraci and Ş. Erkoç, J. Phys. Condens. Matter **7**, 8487 (1995).
[7] L. A. Girifalco and R. A. Lad, J. Chem. Phys. **25**, 693 (1956).
[8] Jian Ping Lu, X. P. Li, and R. M. Martin, Phys. Rev. Lett. **68**, 1551 (1992); Jian Ping Lu, Phys. Rev. Lett. **79**, 1297 (1997).
[9] T. Hertel, R. E. Walkup, and P. Avouris, Phys. Rev. B **58**, 13 870 (1998); A. Buldum and Jian Ping Lu (to be published).
[10] A. Buldum and S. Ciraci, Phys. Rev. B **55**, 2606 (1997).
[11] Slide-spin motions can be clearly seen in the movie of the simulation at http://www.physics.unc.edu/~jpl/ friction/movie.
[12] R. W. Pastor, B. R. Brooks, and A. Szabo, Mol. Phys. **65**, 1409 (1988).
[13] J. D. Schall and D. W. Brenner (private communication).